

Theranostic nanoparticles for enzyme-activatable fluorescence imaging and photodynamic/chemo dual therapy of triple-negative breast cancer

Jaehee Choi*, Hyunjin Kim*, Yongdoo Choi

Molecular Imaging & Therapy Branch, Division of Convergence Technology, National Cancer Center, Goyang, Gyeonggi-do, Korea

*These authors contributed equally to this work.

Correspondence to: Yongdoo Choi, PhD. Molecular Imaging & Therapy Branch, Division of Convergence Technology, National Cancer Center, 323 Ilsan-ro, Ilsandong-gu, Goyang, Gyeonggi-do, Korea. Email: ydchoi@ncc.re.kr

Background: Triple-negative breast cancer (TNBC) is a highly diverse group of cancers characterized by tumors that does not express estrogen and progesterone receptors, as well as human epidermal growth factor receptor 2 (*HER2*) gene expression. TNBC is associated with poor prognosis due to high rate of recurrence and distance metastasis, lack of response to hormonal or *HER2*-targeted therapies, and partial response to chemotherapy. Hence, development of new therapeutic strategies to overcome such limitations is of great importance. Here we describe the application of photosensitizer-conjugated and camptothecin (CPT)-encapsulated hyaluronic acid (HA) nanoparticles as enzyme-activatable theranostic nanoparticles (EATNP) for near-infrared (NIR) fluorescence imaging and photodynamic/chemo dual therapy of TNBC.

Methods: For the preparation of EATNPs, chlorin e6 (Ce6), a second generation photosensitizer, was covalently conjugated to a monomethoxy poly(ethylene glycol)-grafted HA backbone. Ce6-conjugated HA (Ce6-HA) formed self-assembled nanoparticles (i.e., Ce6-HA NPs) in an aqueous solution. Subsequently, CPT, a topoisomerase 1 inhibitor with remarkable anticancer efficacy but with low water solubility, was encapsulated inside the hydrophobic core of Ce6-HA NPs thereby forming EATNPs.

Results: Fluorescence and singlet oxygen generation (SOG) of EATNPs are quenched in its native state. Treatment of EATNPs with hyaluronidase (HAase) induces enzyme concentration-dependent activation of NIR fluorescence and SOG. Moreover, HAase-mediated degradation of the nanoparticles also triggers the release of CPT from the EATNPs. *In vitro* confocal microscopy and cytotoxicity tests confirmed that EATNPs were efficiently introduced into MDA-MB-231 TNBC cell line, thereby inducing better cytotoxicity than that by free CPT. Additional light irradiation onto the EATNP-treated cells significantly increased therapeutic efficacy in TNBC, which indicates that EATNP plays an important role in enzyme-activated NIR fluorescence imaging and photodynamic/chemo dual therapy of TNBC.

Conclusions: We found that HAase may switch on NIR fluorescence and SOG of EATNPs. Moreover, CPT release from the nanoparticles is triggered by the enzyme HAase. *In vitro* cell study showed potential utility of EATNPs for fluorescence imaging and photodynamic/chemo dual therapy of TNBC.

Keywords: Chemotherapy; fluorescence imaging; photodynamic therapy (PDT); theranostic nanoparticles; triple-negative breast cancer (TNBC)

Submitted Aug 05, 2015. Accepted for publication Aug 27, 2015.

doi: 10.3978/j.issn.2223-4292.2015.08.09

View this article at: <http://dx.doi.org/10.3978/j.issn.2223-4292.2015.08.09>

Introduction

Triple-negative breast cancers (TNBC) are characterized by tumors that does not express estrogen and progesterone receptor, as well as human epidermal growth factor receptor 2 (*HER2*) gene expression (1,2). TNBC patients account for approximately 15% of total breast cancer patients. It is associated with poor prognosis due to high rate of recurrence and distance metastasis, lack of response to hormonal or *HER2*-targeted therapies, and partial response to chemotherapy (3). Therefore, development of new strategies to overcome therapeutic limitations of TNBC is of great importance. In the recent studies, nanomedicine-based chemo/gene dual therapy and chemo/photothermal/gene triple therapy of TNBC showed high potential as a new therapeutic option for TNBC (4,5).

Photodynamic therapy (PDT) using combinations of chemical photosensitizers, light, and molecular oxygen has emerged as an effective therapeutic option for various cancers (6,7). Photosensitizers are considered to be potential theranostic agents as they simultaneously generate fluorescence signals for imaging and singlet oxygen for therapy upon excitation by a specific wavelength of light. However, limited tumor selectivity, unfavorable pharmacokinetics, and prolonged skin photosensitivity of water-insoluble PDT agents have been the main obstacles to their clinical applications. In PDT, most of the anticancer drugs used in chemotherapy show low water solubility and severe side effects due to their poor tumor selectivity. Therefore, various drug delivery systems such as nanoparticles and polymer-drug conjugates have been tried to enhance the specificity of photosensitizers and

chemotherapeutic drugs to cancer sites (8-15).

Here, we propose the application of photosensitizer-conjugated and anticancer drug-loaded polymeric nanoparticles as an enzyme-activatable theranostic nanoparticle (EATNP) for selective near-infrared (NIR) fluorescence imaging and photodynamic/chemo dual therapy of TNBC (Figure 1). For the preparation of EATNPs, chlorin e6 (Ce6), a second generation photosensitizer, was covalently conjugated to a monomethoxy poly(ethylene glycol)-grafted hyaluronic acid (HA) backbone. Ce6-conjugated HA (Ce6-HA) formed self-assembled nanoparticles (i.e., Ce6-HA NPs) in an aqueous solution. Subsequently, camptothecin (CPT), a topoisomerase 1 inhibitor with remarkable anticancer efficacy but with low water solubility (16,17), was encapsulated inside the hydrophobic core of Ce6-HA NPs thereby forming EATNPs. We hypothesized that the aggregated photosensitizers inside EATNPs are optically quenched and therefore its fluorescence and singlet oxygen generation (SOG) are turned off while circulating in the blood. However, the preferential accumulation of the nanoparticles in tumors via enhanced permeability and retention (EPR) effect, followed by endocytosis into cancer cells, might cause degradation of the HA backbones by intracellular hyaluronidase (HAase), resulting in triggered release of both Ce6s and CTPs from the nanoparticles. Subsequent fluorescence emission and SOG of the released Ce6s as well as chemotherapeutic action by the released CPTs may enable not only selective fluorescence detection with high target-to-background ratio but also subsequent photodynamic/chemo dual therapy of TNBC. HA, a linear polysaccharide abundant in the extracellular matrix, is

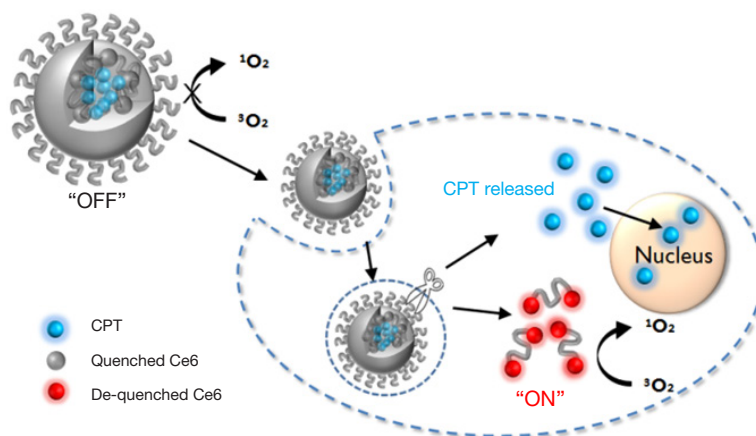


Figure 1 Schematic diagram of enzyme-activatable fluorescence imaging and photodynamic/chemo dual therapy of cancer. CPT, camptothecin; Ce6, chlorin e6.

degradable by tumor-associated enzyme HAdase. Studies have shown positive correlation between the HAdase levels and tumor progressions (18,19); especially HAdase levels of breast metastatic tumors were shown to be 4 times higher than the primary breast cancer tumors (20,21).

Materials and methods

Materials

HA (MW 6.63×10^4 Da) was purchased from Lifecore Biomedical (Chaska, MN, USA). 1-Ethyl-3-(3-dimethylaminopropyl) carbodiimide (EDC), sulfo-N-hydroxysulfosuccinimide (sulfo-NHS), adipic acid dihydrazide (ADH), (S)-(+)-CPT, and HAdase (1,228 unit/mg) were purchased from Sigma-Aldrich (MO, USA). Monomethoxy poly(ethylene glycol)-amine (mPEG-amine, MW =5,000 Da) was purchased from Sunbio (Anyang, Korea). Ce6 and dialysis membranes (MWCO: 10,000 and 50,000 Da) were purchased from Frontier Scientific (UT, USA) and Spectrum Laboratories (CA, USA), respectively. Singlet Oxygen Sensor Green (SOSG) was purchased from Invitrogen (NY, USA). Amicon ultra centrifugal filter tube was obtained from Merk Millipore Corp (Darmstadt, Germany).

The MDA-MB-231 human breast cancer cell line was obtained from the American Type Culture Collection (MD, USA). The cell line was maintained in RPMI 1640 medium (GIBCO®, ThermoFischer Scientific, NY, USA) supplemented with 10% (v/v) fetal bovine serum (FBS) and 1% antibiotic-antimycotic solution in a humidified incubator (37 °C, 5% CO).

Synthesis of Ce6-HA

Ce6-HA was synthesized using a standard EDC/NHS chemistry (Figure 2). At first, amine-functionalized and mPEG-grafted hyaluronic acid (ADH-mPEG-HA) was prepared by conjugating both ADH and mPEG-amine with the carboxylic acids of HA. Briefly, 200 mg HA was dissolved in sodium phosphate buffer (pH 7.4, 20 m); EDC (240 mM, 0.5 mL) and sulfo-NHS (250 mM, 0.5 mL) were sequentially added to the HA solution and stirred for 30 min. Both ADH (27 mg) and mPEG-amine (150 mg) dissolved in sodium phosphate buffer (pH 7.4, 1 mL) and were added to the activated HA solution. The conjugation reaction was allowed to proceed overnight at room temperature. The reactant was dialyzed against deionized

(DI) water for purification and then lyophilized by freeze-drying. Conjugation of ADH and mPEG in a HA polymer backbone was analyzed by $^1\text{H-NMR}$ analysis (Figure S1).

Next, second generation photosensitizer Ce6 was conjugated with ADH-mPEG-HA. At first, the carboxylic acid of Ce6 (34 mg, 1 mL) was activated with EDC (2 mM) and sulfo-NHS (5 mM) in DMSO. Then, ADH-mPEG-HA (122 mg) was dissolved in DMF:H₂O cosolvent (1:1 v/v, 6 mL) and mixed with the activated Ce6 solution, and then conjugation reaction was allowed to proceed overnight at room temperature. Ce6-conjugated mPEG-HA (i.e., Ce6-HA) was purified by dialysis method against phosphate buffer (pH 7.4, 10 mM) and DI water for several times, and then the final product was freeze-dried. The degree of substitution of ADA and mPEG molecules per unit (2 glucose rings) of HA was analyzed with $^1\text{H-NMR}$. To calculate the concentration of Ce6, the absorbance of Ce6-HA (dissolved in 0.1 M NaOH/0.1% SDS) was measured at 400 nm. Ce6 has a molar extinction coefficient of $1.5 \times 10^5 \text{ M}^{-1}\text{cm}^{-1}$ at 400 nm (22,23).

Preparation of CPT-loaded Ce6-HA nanoparticles

Ce6-HA forms self-assembled nanoparticles in aqueous solution during dialysis procedure as it consists of hydrophilic mPEG-grafted HA backbones and hydrophobic Ce6s. Therefore, enzyme-activatable theranostic nanoparticles (EATNP) were prepared by encapsulating anticancer drug CPT with self-assembled Ce6-HA nanoparticles by using the dialysis method. Ce6-HA (9 mg), dissolved in DMF:H₂O (1:1 v/v, 6 mL) cosolvent, was mixed with CPT (1 mg, 200 μL DMSO) and stirred for 1 h for complete dissolution. Then, the solution underwent dialysis against DI water to form self-assembled nanoparticles. Ce6-HA nanoparticles without CPT (i.e., Ce6-HA) were also prepared by dialysis method for comparison. Final products were freeze-dried and preserved at refrigerator for further use.

UV/Vis absorption spectra of Ce6-HA NPs and EATNPs were analyzed by UV/Vis spectrophotometry (DU730, Beckman Coulter, Brea, CA, USA). The hydrodynamic size of CPT/Ce6-HA NPs and Ce6-HA NPs were characterized using a zeta potential/particle sizer (Malvern Instrument, Malvern, UK). The CPT/Ce6-HA NPs were dispersed in phosphate buffered saline (PBS) (6.7 mM, pH 7.4, NaCl 154 mM) and free Ce6 was dissolved in 0.1 M NaOH/ 0.1% SDS solution to analyze the optical characters. Fluorescence spectra were recorded on a multifunctional microplate (Tecan, Safire 2, Switzerland) with excitation at 400 nm.

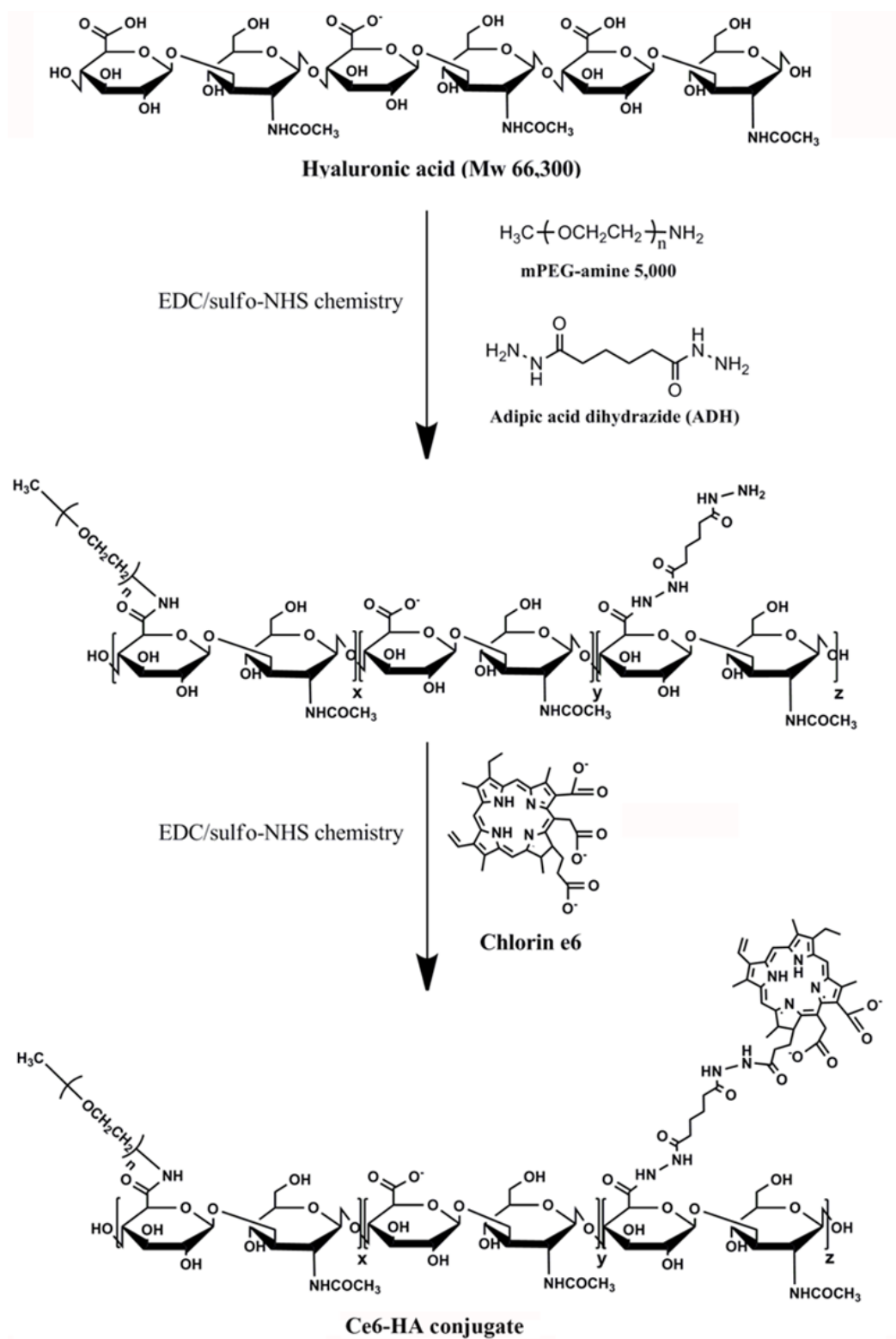


Figure 2 Synthesis of enzyme-activatable theranostic nanoparticles (EATNPs) by EDC/NHS chemistry. EDC, carbodiimide; NHS, N-hydroxysulfosuccinimide; HA, hyaluronic acid; Ce6-HA, Ce6-conjugated HA.

Analysis of fluorescence and SOG

To observe fluorescence quenching and recovery, free Ce6 was dissolved in 1% (v/v) Tween20/PBS to prevent the self-quenching effect resulting from aggregation. Then EATNPs were dissolved in PBS without Tween20. Degradation of HA backbones by HAdase released Ce6 with an increased HAdase concentration that resulted in the recovery of the fluorescence signal. After the addition of HAdase (0–1,200 unit/mL), the fluorescence response of EATNP solution (1 μ M Ce6 equivalent, 100 μ L) was measured at 120 min (excitation: 400 nm, emission: 430–800 nm).

To evaluate the inhibitory and recovery characteristics with respect to SOG, EATNPs were dispersed in PBS solution (saturated with oxygen gas) and then treated with various concentrations of HAdase for 2 h ($n=4$). Next, singlet-oxygen-detecting-reagent (SOSG) was dissolved in HAdase-treated EATNP solution. The final concentration of SOSG reagent in the test solution was maintained at 1 μ M. Each solution was irradiated with a 670 nm CW laser (irradiation dose rate: 68 mW/cm²). Relative SOG of EATNPs with and without HAdase treatment was analyzed by measuring the increase in SOSG fluorescence during 120 s light illumination with laser.

Drug release test

EATNPs dispersed in PBS solution was mixed with either acetate buffer solution (pH 4.5, 100 mM) or HAdase-contained acetate buffer solution (1,200 U/mL), and then enzyme reaction was carried out at 37 °C for 24 h. At each time point, the sample solutions were collected and transferred to amicon ultra centrifugal filter tube (MWCO 3k), and then centrifuged for 10 min at 14,000 \times g. After addition of Tween20 (1 v/v %), the absorbance (UV/V) of the solution was measured at 365 nm and compared with a standard curve of free CPT to calculate the amount of released CPTs.

In vitro cytotoxicity and phototoxicity test

The cells were seeded onto a 96-well plate at 1×10^4 cells/well and incubated for 24 h. Then, free CPT and EATNPs were diluted in RPMI 1640 culture medium (GIBCO®) containing 10% FBS to obtain different concentrations of 0–20 μ M CPT equivalent (that was corresponding to 0–10 μ M Ce6 equivalent for EATNPs). The culture medium was replaced

with fresh medium containing free CPT or EATNPs, and the cells were incubated for 6 h. Thereafter the cells were washed three times and fresh cell culture medium was added. The cells in the PDT-treated group were irradiated with 670 nm CW laser (dose rate: 50 mW/cm², dose: 10 J/cm²). After incubating the cells for an additional 18 h, viability of cells was analyzed using a CCK-8 solution. Absorbance was measured at 450 nm (reference =650 nm) using a microplate reader (Tecan Safire 2). Untreated control cells served as 100% viable cells and the medium served as the background. Data are expressed as the mean (SD) of four data samples.

Confocal fluorescence images

For confocal images, MDA-MB-231 cells were seeded at a density of 1×10^5 cells/well onto a LabTek II Chambered Coverglass (ThermoFischer Scientific, NY, USA) and incubated for 24 h for cell attachment. EATNPs were dispersed and diluted with RPMI 1640 medium (GIBCO®) containing 10% FBS to obtain 1 μ M Ce6 equivalent. The cell culture medium was replaced with EATNPs-containing cell culture medium. After incubation for 6 h, the cells were washed three times and were transferred to a fresh culture medium. Fluorescence images of the cells (excitation: 405 nm, emission: 650 nm long-pass filter) were captured using a confocal scanning-laser microscopy (CSLM, ZEISS LSM 510 META).

Results and discussion

Ce6-HA NPs were prepared with Ce6-HA, as mentioned above. Ce6-HA NPs were round shaped as observed using scanning electron microscope (SEM) (*Figure 3*), and its hydrodynamic size and zeta potential were 170.9 ± 34.67 nm and -27.9 ± 5.55 mV, respectively, confirming the formation of self-assembled nanoparticles. Negative zeta potential value of the nanoparticles indicated that the hydrophilic HA backbones are localized at the outer layer of Ce6-HA NPs. Significant broadening of the Soret band region of HA-Ce6 NP UV/V is spectrum (Beckman Coulter, CA, USA) is the hallmark of Ce6 aggregation, and explains fluorescence quenching of HA-Ce6 NPs compared with the free Ce6 at the same equivalent concentration.

Next, CPT-loaded HA-Ce6 NPs (i.e., EATNPs) were prepared by encapsulating hydrophobic CPT drugs with the self-assembled Ce6-HA NPs using dialysis method. Ce6-HA (9 mg) was dissolved in dimethylformamide:H₂O cosolvent (1:1 v/v, 6 mL) and mixed with CPT (1 mg,

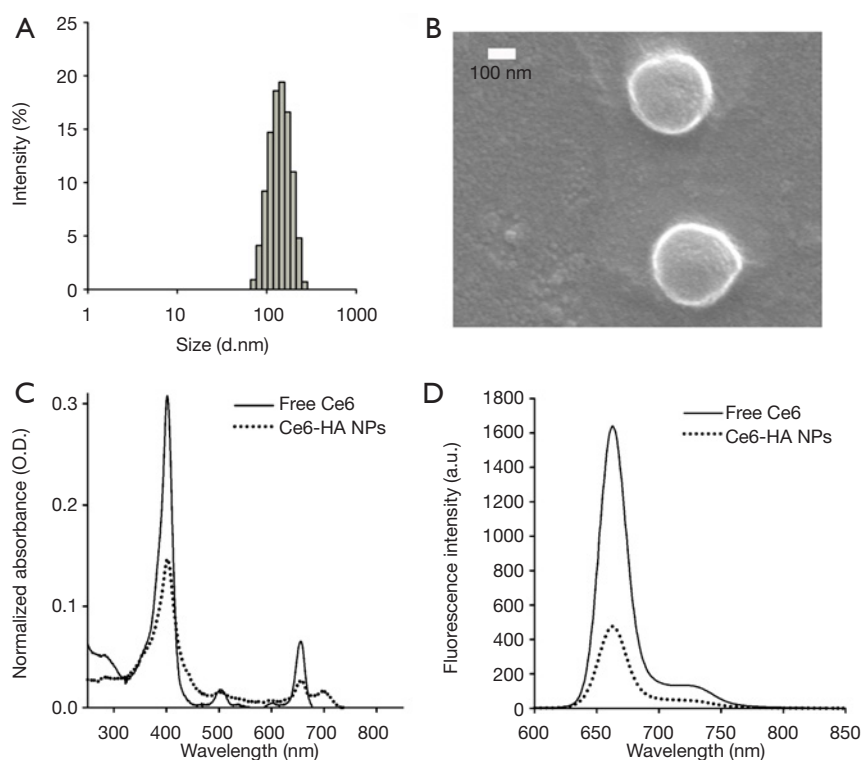


Figure 3 Characterization of Ce6-conjugated HA nanoparticles (Ce6-HA NPs). (A) Hydrodynamic size and (B) scanning electron microscopic (SEM) image of Ce6-HA NPs before encapsulation of CPT; (C) comparison of UV/Vis spectrum and (D) fluorescence intensity with free Ce6 and Ce6-HA NPs at 2 μ M Ce6 equivalent. Ce6, chlorin e6.

200 μ L dimethyl sulfoxide) and stirred for 1 h. Then the solution underwent dialysis against distilled water to form CPT-loaded nanoparticles. The hydrodynamic size and zeta potential of the prepared EATNPs in aqueous solution were 88.78 ± 6.49 nm and -25.4 ± 4.48 mV, respectively. Hydrodynamic size of EATNPs was about two times smaller than Ce6-HA NPs, while its zeta potential value was slightly higher than that of Ce6-HA NPs. Hydrophobic interactions between Ce6s and CPTs inside the nanoparticles tighten the core of the self-assembled nanoparticles, thereby reducing its hydrodynamic size (Figure 4A). Fluorescence of CPT as well as Ce6 was significantly quenched inside EATNPs as shown in Figure 4B (inset image).

As mentioned above, HAdase are overexpressed in various tumors and its levels are much higher in breast metastatic tumors than the primary breast tumors (20,21), indicating that HAdase might be used as a molecular switch for selective imaging and therapy of metastatic TNBCs. Therefore, we confirmed whether treatment of EATNPs with HAdase stimulates recovery of NIR fluorescence and SOG in addition to releasing CTP from the nanoparticles.

NIR fluorescence intensity of EATNPs increased with increasing concentration of HAdase, indicating degradation of the nanoparticle by HAdase and subsequent recovery of Ce6 fluorescence, as shown in Figure 5A,B. The fluorescence intensity of EATNPs was three-fold higher than that of buffer-treated nanoparticles when treated with 1,200 unit/mL HAdase. Then, SOG from EAPNPs was measured in the absence and presence of HAdase, using SOG as a singlet-oxygen-detecting reagent (Figure 5C,D). As in the fluorescence experiment, treatment with HAdase triggered enzyme concentration-dependent recovery of SOG. About 4.1-fold increase in SOG was obtained by treatment with 1,200 unit/mL HAdase.

We tested the effect of HAdase on CPT release from the EATNPs (Figure 6A). In the absence of HAdase, only 17% and 29% of CPT were released from the nanoparticles at 6 h and 24 h, respectively. In contrast, treatment with HAdase (i.e., 1,200 unit/mL) induced 51% release of CPT within 6 h, which is about three times higher than that of non-enzyme treated control. After 24 h of HAdase treatment 58% CPT was released from EATNPs. This

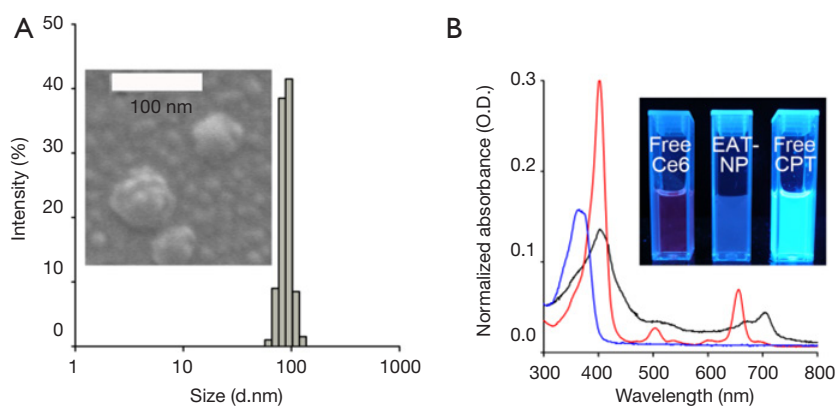


Figure 4 Characterization of EATNP. (A) Hydrodynamic size distribution and scanning electron microscopic (SEM) image of enzyme-activatable theranostic nanoparticle (EATNP); (B) comparison of UV/Vis absorption spectra of free Ce6 (red), EATNP (black), and free CPT (blue) at 2 μ M Ce6 and 5 μ M CPT equivalent concentrations. Inset image: Fluorescence images of free Ce6, EATNPs, and free CPT in aqueous solutions under 380 nm UV light. Ce6, chlorin e6; CPT, camptothecin.

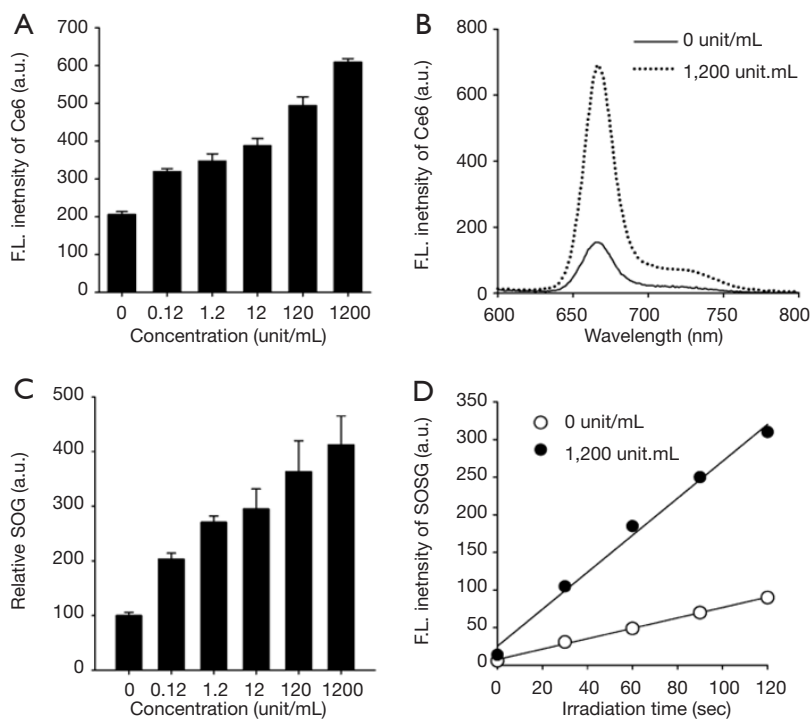


Figure 5 HADase-mediated recovery of fluorescence and SOG of EATNP. (A) Fluorescence intensity of enzyme-activatable theranostic nanoparticles (EATNPs) (1 μ M Ce6 equivalent) measured after 2 h of HADase treatment at various concentrations; (B) fluorescence spectra of EATNPs (1 μ M Ce6 equivalent) treated with buffer solution or HADase (1,200 unit/mL) for 2 h; (C) relative SOG *vs.* HADase concentration. EATNPs were treated with HADase at various concentrations and then SOG of the EATNPs was measured after laser irradiation (670 nm laser); (D) time-dependent SOG of HADase-treated EATNPs during irradiation (670 nm CW laser, 68 mW/cm², n=4). Ce6, chlorin e6; SOG, singlet oxygen generation.

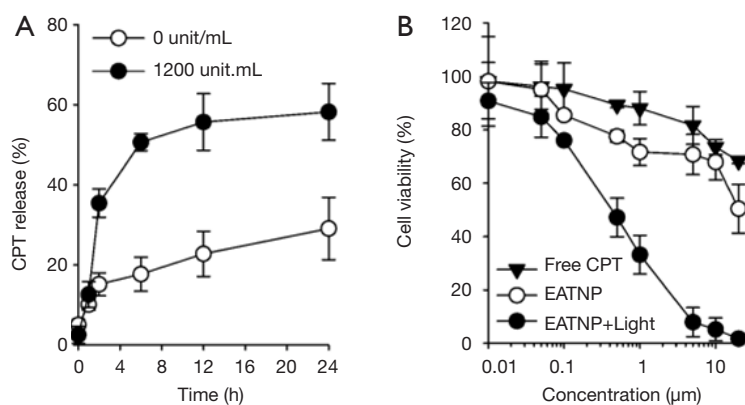


Figure 6 HADase-activatable drug release and PDT effect. (A) HADase-dependent release profile of CPT from enzyme-activatable theranostic nanoparticles (EATNPs) (2 μ M CPT equivalent, n=4); (B) viability of MDA-MB-231 cells after treatment with free CPT and EATNP at various concentrations of CPT equivalent (n=4). CPT, camptothecin.

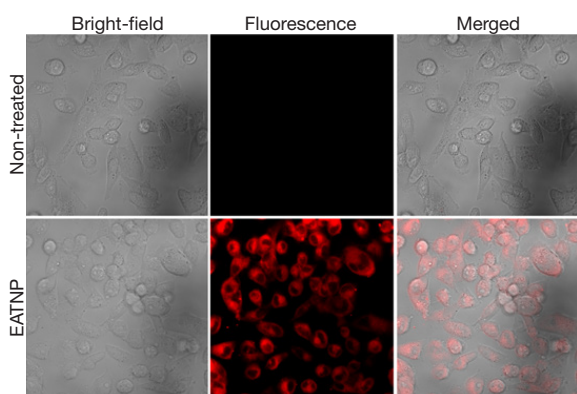


Figure 7 Confocal laser fluorescence images (Ex. 405 nm, Em. 650 nm long-pass filter) of the cells treated with cell culture media and enzyme-activatable theranostic nanoparticles (EATNP) (1 μ M Ce6 equivalent) for 6 h. Red colour indicates fluorescence signals from Ce6 inside the cells. Ce6, chlorin e6.

data matched well with fluorescence recovery of HADase-treated EATNPs indicating HADase-mediated nanoparticle degradation and subsequent release of both Ce6s and CTPs.

We then evaluated the therapeutic efficacy of EATNPs in TNBC cell line, MDA-MB-231 cells (Figure 6B). The cells were treated with free CPT and EATNPs at various concentration of CPT equivalent for 6 h and washed three times with fresh cell culture media. MDA-MB-231 cells in the EATNP plus light group additionally received light irradiation with a 670 nm CW laser (dose rate: 68 mW/cm², dose: 10 J/cm²). After incubating the cells for an additional 18 h, viability of the cells was analyzed. As a result, about 28% of the cells were dead after treating the cells with EATNPs at 1 μ M CPT equivalent, while 12%

of cell death was recorded with free CPT treatment at the same concentration. Upon additional light illumination for PDT, 67% of the cells were killed. Also, cell viability of the EATNP plus light group (20 μ M CPT equivalent) was reduced to 2%, while cell viability of EATNP- and free CPT-treated groups were 50% and 68%, respectively.

Strong fluorescence signals of the EATNP-treated cells were observed in the images obtained using a confocal laser scanning microscope, which may indicate efficient cellular uptake of EATNPs by the cells and fluorescence recovery inside the cells (Figure 7).

Conclusions

In summary, we found that HADase may switch on NIR fluorescence and SOG of EATNPs. Moreover, CTP release from the nanoparticles is triggered by the enzyme HADase. *In vitro* cell study showed potential utility of EATNPs for fluorescence imaging and photodynamic/chemo dual therapy of TNBC.

Acknowledgements

Funding: This work was supported by the National Research Foundation of Korea (NRF) grant (NRF-2014R1A2A1A11050923) funded by the Korea government (MSIP), and by a National Cancer Center grant (1310160), Republic of Korea.

Footnote

Conflicts of Interest: The authors have no conflicts of interest

to declare.

References

- Davis SL, Eckhardt SG, Tentler JJ, Diamond JR. Triple-negative breast cancer: bridging the gap from cancer genomics to predictive biomarkers. *Ther Adv Med Oncol* 2014;6:88-100.
- Oakman C, Viale G, Di Leo A. Management of triple negative breast cancer. *Breast* 2010;19:312-21.
- Wahba HA, El-Hadaad HA. Current approaches in treatment of triple-negative breast cancer. *Cancer Biol Med* 2015;12:106-16.
- Deng ZJ, Morton SW, Ben-Akiva E, Dreaden EC, Shopsowitz KE, Hammond PT. Layer-by-layer nanoparticles for systemic codelivery of an anticancer drug and siRNA for potential triple-negative breast cancer treatment. *ACS Nano* 2013;7:9571-84.
- Su S, Tian Y, Li Y, Ding Y, Ji T, Wu M, Wu Y, Nie G. "Triple-punch" strategy for triple negative breast cancer therapy with minimized drug dosage and improved antitumor efficacy. *ACS Nano* 2015;9:1367-78.
- Celli JP, Spring BQ, Rizvi I, Evans CL, Samkoe KS, Verma S, Pogue BW, Hasan T. Imaging and photodynamic therapy: mechanisms, monitoring, and optimization. *Chem Rev* 2010;110:2795-838.
- Josefsen LB, Boyle RW. Unique diagnostic and therapeutic roles of porphyrins and phthalocyanines in photodynamic therapy, imaging and theranostics. *Theranostics* 2012;2:916-66.
- Pérez-Herrero E, Fernández-Medarde A. Advanced targeted therapies in cancer: Drug nanocarriers, the future of chemotherapy. *Eur J Pharm Biopharm* 2015;93:52-79.
- Mohamed S, Parayath NN, Taurin S, Greish K. Polymeric nano-micelles: versatile platform for targeted delivery in cancer. *Ther Deliv* 2014;5:1101-21.
- Park D, Cho Y, Goh SH, Choi Y. Hyaluronic acid-polyppyrrrole nanoparticles as pH-responsive theranostics. *Chem Commun (Camb)* 2014;50:15014-7.
- Canal F, Sanchis J, Vicent MJ. Polymer--drug conjugates as nano-sized medicines. *Curr Opin Biotechnol* 2011;22:894-900.
- Jang B, Park JY, Tung CH, Kim IH, Choi Y. Gold nanorod-photosensitizer complex for near-infrared fluorescence imaging and photodynamic/photothermal therapy in vivo. *ACS Nano* 2011;5:1086-94.
- Cho Y, Kim H, Choi Y. A graphene oxide-photosensitizer complex as an enzyme-activatable theranostic agent. *Chem Commun (Camb)* 2013;49:1202-4.
- Wang YG, Kim H, Mun S, Kim D, Choi Y. Indocyanine green-loaded perfluorocarbon nanoemulsions for bimodal (19)F-magnetic resonance/nearinfrared fluorescence imaging and subsequent phototherapy. *Quant Imaging Med Surg* 2013;3:132-40.
- Kim J, Tung CH, Choi Y. Smart dual-functional warhead for folate receptor-specific activatable imaging and photodynamic therapy. *Chem Commun (Camb)* 2014;50:10600-3.
- Liu YQ, Li WQ, Morris-Natschke SL, Qian K, Yang L, Zhu GX, Wu XB, Chen AL, Zhang SY, Nan X, Lee KH. Perspectives on biologically active camptothecin derivatives. *Med Res Rev* 2015;35:753-89.
- Yokoyama M, Opanasopit P, Okano T, Kawano K, Maitani Y. Polymer design and incorporation methods for polymeric micelle carrier system containing water-insoluble anti-cancer agent camptothecin. *J Drug Target* 2004;12:373-84.
- Choi KY, Saravanakumar G, Park JH, Park K. Hyaluronic acid-based nanocarriers for intracellular targeting: interfacial interactions with proteins in cancer. *Colloids Surf B Biointerfaces* 2012;99:82-94.
- Beech DJ, Madan AK, Deng N. Expression of PH-20 in normal and neoplastic breast tissue. *J Surg Res* 2002;103:203-7.
- Bertrand P, Girard N, Duval C, d'Anjou J, Chauzy C, Ménard JF, Delpech B. Increased hyaluronidase levels in breast tumor metastases. *Int J Cancer* 1997;73:327-31.
- Udabage L, Brownlee GR, Nilsson SK, Brown TJ. The over-expression of HAS2, Hyal-2 and CD44 is implicated in the invasiveness of breast cancer. *Exp Cell Res* 2005;310:205-17.
- Hamblin MR, Miller JL, Rizvi I, Ortel B, Maytin EV, Hasan T. Pegylation of a chlorin(e6) polymer conjugate increases tumor targeting of photosensitizer. *Cancer Res* 2001;61:7155-62.
- Kim H, Mun s, Choi Y. Photosensitizer-conjugated polymeric nanoparticles for redox-responsive fluorescence imaging and photodynamic therapy. *J Mater Chem B* 2013;1:429-31.

Cite this article as: Choi J, Kim H, Choi Y. Theranostic nanoparticles for enzyme-activatable fluorescence imaging and photodynamic/chemo dual therapy of triple-negative breast cancer. *Quant Imaging Med Surg* 2015;5(5):656-664. doi: 10.3978/j.issn.2223-4292.2015.08.09

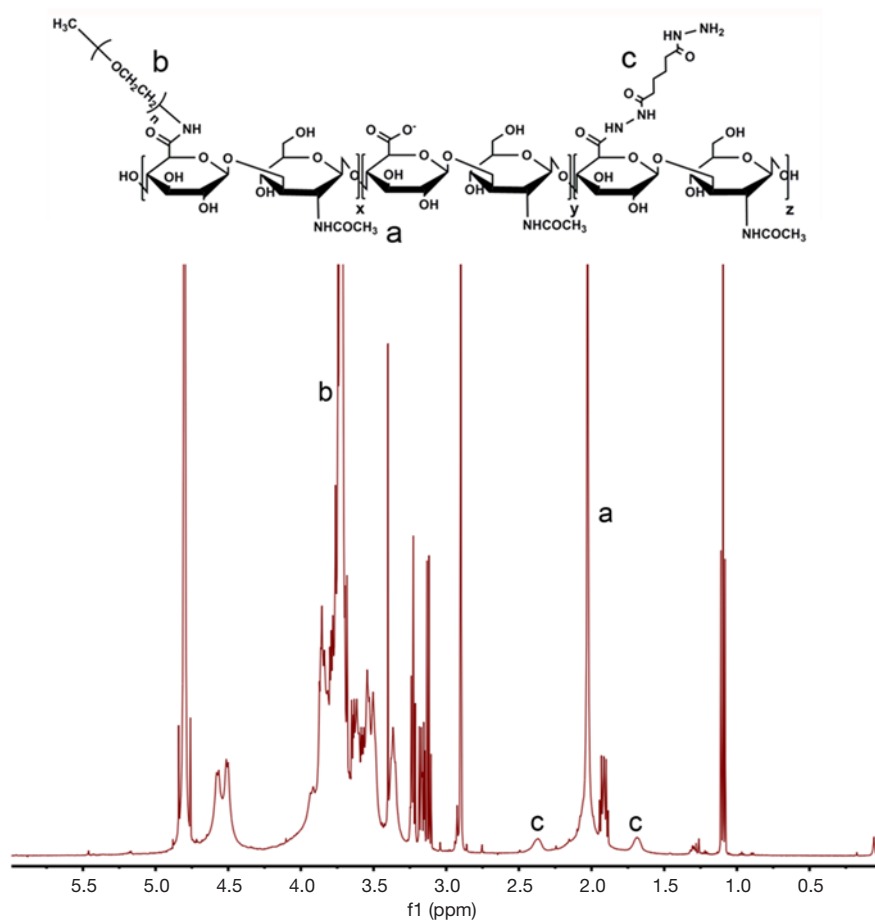


Figure S1 ¹H-NMR spectra of ADH-mPEG-HA conjugates in D₂O/DMSO-d₆ cosolvent (1:1 v/v). The protons of the acetamido methyl group of the HA backbone, -OCH₂CH₂- group of mPEG, and -CH₂CH₂- of ADH were observed at 2.03 ppm (a), 3.72 ppm (b), and 1.69 and 2.37 ppm (c), respectively. The ¹H-NMR spectrum of ADH-mPEG-HA conjugates confirmed the successful conjugation of mPEG and ADH onto the HA backbones. ADH-mPEG-HA, amine-functionalized and mPEG-grafted hyaluronic acid.